Special Section: UZIG USGS
Vadose Zone Journal

Transport of Tritium Contamination to the Atmosphere in an Arid Environment

C. A. Garcia,* B. J. Andraski, D. A. Stonestrom, C. A. Cooper, M. J. Johnson, R. L. Michel, and S. W. Wheatcraft

Soil–plant–atmosphere interactions strongly influence water movement in desert unsaturated zones, but little is known about how such interactions affect atmospheric release of subsurface water-borne contaminants. This 2-yr study, performed at the U.S. Geological Survey's Amargosa Desert Research Site in southern Nevada, quantified the magnitude and spatiotemporal variability of tritium (^{3}H) transport from the shallow unsaturated zone to the atmosphere adjacent to a low-level radioactive waste (LLRW) facility. Tritium fluxes were calculated as the product of ^{3}H concentrations in water vapor and respective evaporation and transpiration water-vapor fluxes. Quarterly measured ^{3}H concentrations in soil water vapor and in leaf water of the dominant creosote-bush [*Larrea tridentata* (DC.) Coville] were spatially extrapolated and temporally interpolated to develop daily maps of contamination across the 0.76-km^2 study area. Maximum plant and root-zone soil concentrations (4200 and 8700 Bq L^{-1}, respectively) were measured 25 m from the LLRW facility boundary. Continuous evaporation was estimated using a Priestley–Taylor model and transpiration was computed as the difference between measured eddy-covariance evapotranspiration and estimated evaporation. The mean evaporation/transpiration ratio was 3:1. Tritium released from the study area ranged from 0.12 to 12 μg d^{-1} and totaled 1.5 mg (8.2 × 10^{10} Bq) over 2 yr. Tritium flux variability was driven spatially by proximity to ^{3}H source areas and temporally by changes in ^{3}H concentrations and in the partitioning between evaporation and transpiration. Evapotranspiration removed and limited penetration of precipitation beneath native vegetation and fostered upward movement and release of ^{3}H from below the root zone.

Abbreviations: ADRS, Amargosa Desert Research Site; ET, evapotranspiration; ^{3}H, tritium; ^{3}HHO, tritiated water; LLRW, low-level radioactive waste.

Desert plants strongly influence water movement in arid unsaturated zones, but little is known about the remediation potential of desert vegetation with regard to water-borne contaminants. In the arid western United States, where low moisture levels and high temperature gradients promote vapor-phase transport in near-surface soils (Scanlon and Milly, 1994), the effects of evapotranspiration (ET) on radionuclide transport and fate near waste disposal facilities is of particular concern. Tritium (^{3}H), the radioactive isotope of H (half-life of 12.32 yr), comprises a large portion of radionuclide activity disposed at waste facilities. Because water (H_2O) and tritiated water (^{3}HHO) share similar chemical and transport properties, primary ^{3}H migration pathways follow soil water and vapor (Phillips, 1994). Studies at the USGS's Amargosa Desert Research Site (ADRS) have found that tritiated water vapor ($^3HHO_v$) moves preferentially from the LLRW source through coarse-textured sediment layers (Andraski et al., 2005; Mayers et al., 2005).

Previous studies have shown that desert plants have a considerable influence on water flow processes in shallow soils and thick unsaturated zones. One- to 12-yr field studies by Fischer (1992), Andraski (1997b), and Scanlon et al. (2003) and numerical modeling by Walvoord et al. (2002), Scanlon et al. (2003), and Kwicklis et al. (2006) indicated that desert unsaturated zones beneath sparse vegetation in the arid western United States are dominated by low water potentials and upward hydraulic gradients. These upward gradients reflect unsaturated zone drying conditions established in response to paleoclimate change and a shift from mesic to xeric vegetation that occurred about 10,000 to 20,000 yr ago (Walvoord et al., 2004).

Plants also play an important role in the detection and mapping of subsurface contaminants, and phreatophytes have been used to remediate contaminated groundwater. Researchers have used plants to detect subsurface liquid tritiated water ($^3HHO_w$) and $^3HHO_v$ contamination (Kalisz et al., 1988; Rickard and Kirby, 1987; Rickard and Price, 1989; Andraski et al., 2003), to map $^3HHO_v$ concentrations within and below the soil root zone (Andraski et al., 2005), and to remediate a tritiated groundwater plume (Negri et al., 2000). While the use of phreatophytes to hydraulically control and remediate groundwater in humid settings has been documented, the phytoremediation potential of desert plants in environments with thick unsaturated zones has yet to be quantified.

Current research at the ADRS has centered on identifying, mapping, and modeling subsurface ^{3}H contamination and

C.A. Garcia, B.J. Andraski, and M.J. Johnson, U.S. Geological Survey, 2730 N. Deer Run Rd., Carson City, NV 89701; D.A. Stonestrom and R.L. Michel, U.S. Geological Survey, 345 Middlefield Rd., Menlo Park, CA 94025; C.A. Cooper, Desert Research Institute, 2215 Raggio Pkwy., Reno, NV 89512; and S.W. Wheatcraft, Dep. of Geological Sciences, Univ. of Nevada, Reno, NV 89557. Received 4 Feb. 2008. *Corresponding author (cgarcia@usgs.gov).

Vadose Zone J. 8:450–461
doi:10.2136/vzj2008.0022

© Soil Science Society of America
677 S. Segoe Rd. Madison, WI 53711 USA.
All rights reserved. No part of this periodical may be reproduced or transmitted in any form or by any means, electronic or mechanical, including photocopying, recording, or any information storage and retrieval system, without permission in writing from the publisher.

transport from the waste facility (Striegl et al., 1996; Andraski et al., 2005; Mayers et al., 2005). Andraski et al. (2005) documented the importance of native vegetation on the vertical subsurface migration of $^3HHO_v$ adjacent to the LLRW facility and showed that beneath vegetation, the total flux was dominated by an upward diffusive $^3HHO_v$ flux from the sub-root zone to the root zone; however, transport of ^3H from the subsurface to the atmosphere and the effects of meteorological variability on vertical transport have not been investigated in detail.

The objective of this study was to quantify the ^3H flux from the shallow unsaturated zone to the atmosphere beneath a sparsely vegetated area adjacent to a LLRW facility. The spatial and temporal variability of upward ^3H transport was defined on the basis of 2 yr of continuously measured ET fluxes and quarterly measured plant and soil concentrations.

Materials and Methods

Site Description

The ADRS and adjacent waste-burial facility are in the Mojave Desert, 17 km south of Beatty, NV, and 20 km east of Death Valley National Park (Fig. 1). The ADRS is in one of the most arid regions of the United States. Precipitation averaged 130 mm yr^{-1} during 2001 to 2005 and was highly variable from month to month and year to year (Johnson et al., 2007). Annual potential evaporation (*E*) is roughly 1900 mm (Nichols, 1987). The Amargosa Desert, in the Basin and Range Province, is bounded by Paleozoic rock and Tertiary volcanic rock mountains (Fischer, 1992). Surface soils are mapped as the Yermo (loamy-skeletal, mixed, superactive, calcareous, thermic Typic Torriorthents)–Arizo (sandy-skeletal, mixed, thermic Typic Torriorthents) association. Subsurface sediments are predominantly fluvial deposits, consisting of several sand and gravel sequences. Andraski (1996) provided additional information on soil properties at the study site. Depth to the water table ranges from 85 to 115 m below the land surface

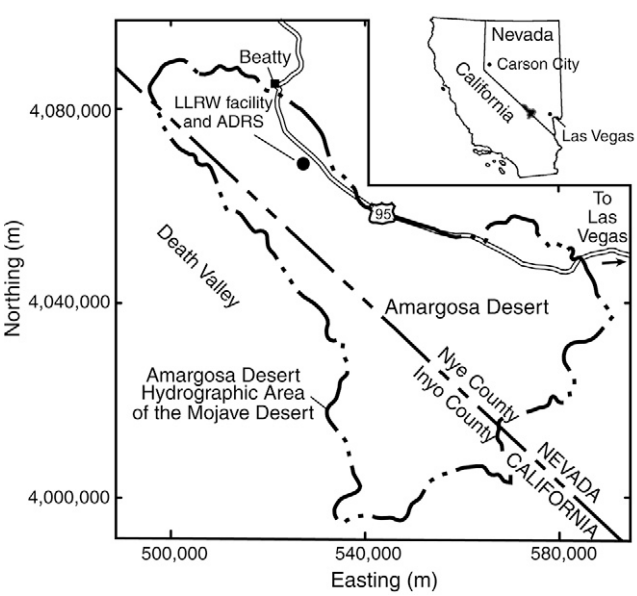

FIG. 1. Location map showing the low-level radioactive waste (LLRW) facility and the Amargosa Desert Research Site (ADRS) near Beatty, NV. Base from USGS digital data (Universal Transverse Mercator projection, Zone 11, North American Datum of 1983).

(Fischer, 1992). The sparsely vegetated study site is dominated by creosote-bush, an evergreen shrub (Smith et al., 1997). The root system of creosote-bush can exceed 4 m radially (Gile et al., 1998) and rooting depth generally corresponds with the penetration depth of maximum annual precipitation, about 0.75 to 1 m at the ADRS (Andraski, 1997b). Root-zone soil water content ranges from 0.02 to 0.12 $m^3\ m^{-3}$ while sub-root-zone gravelly sand (~1–2-m depth) water contents show little variability, averaging 0.05 ± 0.009 $m^3\ m^{-3}$ (2001–2005; Johnson et al., 2007). Plant transpiration (*T*), soil *E*, and the capillary break formed by the interface between the sand and gravel layer and the overlying finer textured root-zone soil inhibit deeper percolation of precipitation (Fischer, 1992; Andraski, 1997a).

The waste facility formerly disposed of LLRW (1962–1992) and continues to dispose of hazardous chemical waste (1970–present). Radioactive wastes were buried in more than 20 unlined trenches ranging from 2 to 15 m deep (Fischer, 1992; Andraski, 1997b). Of the nearly 400 radionuclides disposed at the site, the most common was ^3H (58% of the total activity). A total ^3H activity of approximately 1.27×10^{16} Bq (equivalent to ~240,000 mg of ^3HHO; 1 Bq = 27 pCi) was disposed at the site (Nevada State Health Division, unpublished data, 1992). Waste forms included solids in metal drums, concrete casks, and wooden and cardboard boxes. Although disposal of liquid waste required solidification with Portland cement before trench emplacement, a 1976 U.S. Nuclear Regulatory Commission investigation reported that liquid waste delivered between 1962 and 1975 was disposed directly into the trenches (U.S. Nuclear Regulatory Commission, 1976). Striegl et al. (1996) estimated the associated liquid waste volume at nearly 3000 m^3. Thus, ^3H in the waste source is probably a mixture of $^3HHO_w$ in the liquid waste and both organic and inorganic dissolved, sorbed, and solid phases of ^3H (Striegl et al., 1996).

Field Data Sampling and Analysis

Tritium fluxes from the subsurface to the atmosphere were computed as the product of $^3HHO_v$ concentrations and evaporation and transpiration fluxes. Measured concentrations in plants and root-zone soil were used to estimate the magnitude, distribution, and temporal variability of ^3H contamination. Evapotranspiration was measured continuously and bare-soil *E*, soil moisture, net radiation, and ground heat flux data were used to partition ET into continuous soil *E* and plant *T*.

Tritiated Water Vapor Concentrations

Concentrations of $^3HHO_v$ in soil, canopy air, and plants were determined quarterly from August 2003 to August 2005 along two transects shown in Fig. 2. Soil water vapor and within-canopy air samples were collected using vapor extraction methods described by Striegl (1988) and Andraski et al. (2003). Soil gas tubes were installed to nominal depths of 50 and 150 cm; water vapor samples pulled from these depths are assumed to yield values of $^3HHO_v$ representative of the root-zone soil and sub-root-zone gravelly sand, respectively. Soil water vapor and canopy air samples were collected every quarter at sites 25, 200, and 400 m from the LLRW facility. Annually, soil water vapor samples also were collected at sites 0, 100, 300, and 3000 m (distant study site) from the LLRW facility, and a canopy air sample was collected at the distant study site. Plant samples were collected from

creosote-bush foliage (Andraski et al., 2003). The same replicate plants (n = 2) were sampled quarterly at each transect site with the exception of the 0-m sites, which had no plants.

Plant water extractions were performed using azeotropic distillation with toluene (Revesz and Woods, 1990). In contrast with previous work at the site that relied on solar distillation of plant water, our study used toluene extraction because it required collection of a smaller mass of foliage from the repeatedly sampled plants (i.e., 20 vs. 200 g). Soil water vapor, canopy air, and plant water samples were analyzed for ^{3}H using liquid scintillation counting described by Thatcher et al. (1977) at the USGS isotope laboratory in Menlo Park, CA. For the purpose of computing the ^{3}H flux from plants to the atmosphere, plant $^3HHO_w$ concentrations were converted to $^3HHO_v$ concentrations using an equilibrium ^{3}H isotope fractionation factor (Ferronsky and Polyakov, 1982) that was adjusted for the average air temperature on the day of sample collection.

The effect of location (distance from the waste facility) on plant $^3HHO_v$ concentrations within a given transect and quarter was tested using ANOVA procedures (SAS Institute, 2001) and means were compared using Fisher's LSD (Steel and Torrie, 1980). The P = 0.05 significance level was used for these statistical tests. Before applying ANOVA procedures, differences between observed values and model predictions (Shapiro–Wilk W statistic and residual plots; Fernandez, 1992) were used to test the assumptions of normally distributed and homogenous error, and to determine the need for data transformation.

Quarterly and daily maps of plant and root-zone soil $^3HHO_v$ concentrations across the complete study area were developed by combining our quarterly transect data with contaminant distribution results reported by Andraski et al. (2005). The Andraski et al. (2005) study used a single synoptic sampling (May 2001) of soil gas along with solar distillation of plant water from many sites (n = 103); ordinary kriging was used to develop a plant $^3HHO_w$ map (25- by 25-m cell size, 1211 cells). An associated root-zone soil $^3HHO_v$ map was generated using a linear regression relation between ^{3}H in plant water and ^{3}H in soil water vapor at 10 locations (r^2 = 0.96). For the present study, the May 2001 root-zone soil $^3HHO_v$ map served directly as a base map for delineating soil concentrations; a plant $^3HHO_v$ base map was developed by converting the May 2001 solar-distilled plant $^3HHO_w$ map concentrations to toluene-extracted plant $^3HHO_v$ concentrations using a linear regression equation (r^2 = 0.997) and the equilibrium ^{3}H isotope fractionation factor. For each quarter, a map of plant $^3HHO_v$ concentrations was generated by (i) developing a linear regression equation that related quarterly plant data to May 2001 plant data collected at common sampling sites ($r^2 \geq 0.956$) and (ii) applying that equation to the May 2001 base map. Quarterly maps of root-zone soil $^3HHO_v$ concentrations were generated using the same procedures ($r^2 \geq 0.886$). Daily maps of plant and soil $^3HHO_v$ concentrations were generated by interpolating quarterly map results on a cell by cell basis (n = 1211). Further details on contaminant mapping have been provided by Garcia (2007).

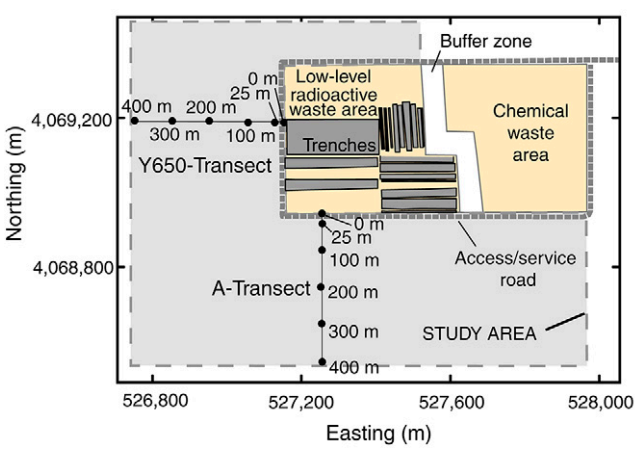

FIG. 2. Amargosa Desert Research Site Y650 and A sampling transects within the 0.76-km^2 study area adjacent to the waste disposal facility. Not shown is the distant study site located about 3 km south of the waste facility (easting 528,141 m, northing 4,065,820 m).

Evaporation and Transpiration

Continuous ET was measured using the eddy-covariance method (Johnson et al., 2007). To quantify the ^{3}H flux from the subsurface to the atmosphere using measured $^3HHO_v$ concentrations in plants and root-zone soil, ET was partitioned into bare-soil E and plant T. Continuous E and T were estimated using the following one-layer, two-component (bare soil and plant canopy) model modified from Stannard (1988):

$$\mathrm{ET} = \mathrm{Fc}_s E_{ss} + (1 - \mathrm{Fc}_s) T_{ss} \quad [1]$$

$$E = \mathrm{Fc}_s E_{ss} \quad [2]$$

$$T = (1 - \mathrm{Fc}_s) T_{ss} \quad [3]$$

where ET is the landscape-scale (eddy-covariance measured) ET (g m^{-2} d^{-1}; 1.0 g m^{-2} d^{-1} = 0.001 mm d^{-1}), Fc_s is the fractional cover of bare soil across the study area (unitless), E_{ss} is the site-scale E estimated from a calibrated Priestley–Taylor model (Priestley and Taylor, 1972) (g m^{-2} d^{-1}), T_{ss} is the site-scale T (g m^{-2} d^{-1}), E is the landscape-scale E (g m^{-2} d^{-1}), and T is the landscape-scale T estimated as the difference between ET and E (g m^{-2} d^{-1}). The fractional cover of bare soil and all plants (1 – Fc_s) across the landscape, ranging from 0 (no cover) to 1 (full cover), was measured using the line-transect method (Smith, 1974). Four, 200-m transects extending northwest, northeast, southwest, and southeast from the eddy-covariance station were measured quarterly; the transect area represents nearly 20% of the 0.76-km^2 study area. Plant cover was estimated from additive measurements of the vertical projection of green (nondormant) plant canopies overlying line transects. Bare soil cover included gaps between plants and within plant canopies. The Fc_s was computed as the total coverage of bare soil for all four transects divided by the total transect length (800 m). Quarterly measured transect data were interpolated over time to develop a continuous Fc_s data set. Evaporation estimates were based on the Priestley–Taylor model, which was calibrated using periodic, 1-m-diameter, hemispherical chamber measurements of evaporation and continuously measured micrometeorological data (see Appendix A). Comparisons between eddy-covariance and periodic hemispherical chamber ET measurements validated the use of the chamber to partition continuously measured eddy-covariance ET into E and T (see Appendix B).

Tritium Flux

Tritium fluxes from the shallow unsaturated zone to the atmosphere adjacent to the waste facility (Fig. 2) were calculated using mapped $^3HHO_v$ concentration distributions together with E and T fluxes within the 0.76-km^2 study area. Daily ^3H fluxes were computed using the following equation:

$$J = EX_s + TX_p \quad [4]$$

where J is the ^3H flux (g m^{-2} d^{-1}) and X is the mass fraction of ^3H in root-zone soil (s) and plant (p) vapor (unitless). Mass fractions were computed from soil and plant $^3HHO_v$ concentration distributions using a general equation for converting measured ^3H activities, expressed as absolute concentrations, to mass fractions in aqueous systems (Stonestrom et al., personal communication, 2006):

$$X = 2.22293 \times 10^{-18} Y \quad [5]$$

where Y is the $^3HHO_v$ concentration in tritium units (1 tritium unit = 0.1184 Bq L^{-1}). As a first approximation, complications due to individual concentration gradients among gases (including isotopically distinct species of the same gas) were not considered in the analysis (Thorstenson and Pollock, 1989; Evans et al., 2001). Instead, ^3H fluxes were approximated as simple products of ET fluxes and ^3H concentrations. In addition, evaporative fluxes beneath plant canopies were assumed negligible and the potential effects of barometric pumping (Auer et al., 1996) were not considered. Although barometric pumping processes are important with respect to diffusion modeling, they were assumed here to produce only second-order effects with respect to the estimated fluxes.

Plant sampling focused on creosote-bush because of its dominance in the plant community and because its evergreen character provided sufficient foliage for repeat sampling throughout the year. Concentration differences among plant species and diurnal variations of $^3HHO_w$ concentrations in creosote-bush were assumed negligible. Fractional cover data in Table 1 indicate that, in accordance with their drought-deciduous character, shadscale [*Atriplex confertifolia* (Torr. & Frém.) S. Watson], burrobush [*Ambrosia dumosa* (Gray) Payne], and wolfberry (*Lycium pallidum* Miers) periodically contributed to the plant ^3H flux. Analysis of variance statistics confirm, however, that $^3HHO_w$ concentrations in creosote-bush and other plant species measured in April 2006 were not significantly different ($P > F = 0.61$; Garcia, 2007). Creosote-bush foliage samples for a given quarter often were collected during the afternoon of 1 d and the morning of the next, but the effect of sampling time was assumed to be negligible. This was confirmed by replicate ($n = 2$) test samples collected at three different times (7:40, 12:05, and 14:55 h) during April 2006, which showed that concentrations differed by <10% (CV = 9%; Steel and Torrie, 1980).

Soil Profile Water Content Measurement

Profile water contents were measured quarterly at a vegetated area within the study site using a neutron probe and replicate (n = 3) access tubes (Andraski, 1997b; Johnson et al., 2007). The area was about 100 m west of the A transect and 300 m south of the Y650 transect. Data collected from 15 to 150 cm below the land surface were used to assess general relations between soil moisture and $^3HHO_v$ concentrations in the root zone and sub-root zone.

Results and Discussion

Tritiated Water Vapor Concentration Variability and Trends

Quarterly $^3HHO_v$ concentrations in soil and plants generally decreased as distance from the waste facility increased (Fig. 3). The maximum plant $^3HHO_v$ concentration measured along the Y650 transect was 4200 Bq L^{-1} (August 2004, 25 m from the facility); the maximum along the A transect was 1050 Bq L^{-1} (August 2004, 100 m from the facility). The maximum root-zone

Table 1. Plant community characteristics measured quarterly from August 2003 to August 2005. Canopy area for a given species is the average for all individuals encountered along the four, 200-m long transects; fractional cover is that determined by the line-transect method; and relative dominance is the ratio of fractional cover for a given species to the fractional cover of all species.

Common name	Average canopy area	Fractional cover	Relative dominance
	m^2		%
	August 2003		
Creosote-bush	1.21	0.048	94.25
Shadscale	†	0.000	0.00
Burrobush	0.28	0.003	5.75
Wolfberry	†	0.000	0.00
	October 2003		
Creosote-bush	0.95	0.077	86.98
Shadscale	0.14	0.006	6.72
Burrobush	0.18	0.006	6.30
Wolfberry	†	0.000	0.00
	January 2004		
Creosote-bush	1.14	0.042	85.09
Shadscale	0.14	0.004	7.77
Burrobush	0.15	0.004	7.14
Wolfberry	†	0.000	0.00
	April–May 2004		
Creosote-bush	1.39	0.045	68.54
Shadscale	0.13	0.003	5.25
Burrobush	0.27	0.007	11.32
Wolfberry	1.25	0.010	14.89
	August 2004		
Creosote-bush	1.07	0.044	100.0
Shadscale	†	0.000	0.0
Burrobush	†	0.000	0.0
Wolfberry	†	0.000	0.0
	October 2004		
Creosote-bush	1.12	0.041	100.0
Shadscale	†	0.000	0.0
Burrobush	†	0.000	0.0
Wolfberry	†	0.000	0.0
	January 2005		
Creosote-bush	1.18	0.050	72.9
Shadscale	0.08	0.002	3.4
Burrobush	0.19	0.007	10.8
Wolfberry	1.01	0.009	12.8
	April–May 2005		
Creosote-bush	1.08	0.060	60.2
Shadscale	0.25	0.011	11.4
Burrobush	0.32	0.014	13.7
Wolfberry	1.07	0.015	14.7
	August 2005		
Creosote-bush	0.88	0.039	71.3
Shadscale	0.2	0.005	8.5
Burrobush	0.3	0.010	18.9
Wolfberry	0.42	0.001	1.3

† No measurable canopy.

soil $^3HHO_v$ concentration measured along the Y650 transect was 8700 Bq L^{-1} (August 2003, 25 m from the facility); the maximum along the A transect was 1000 Bq L^{-1} (April–May 2004, 100 m from the facility). A dirt road adjacent to the Y650- and A-transect sample collection sites located 0 and 25 m, respectively, from the facility (Fig. 2) might have led to $^3HHO_v$ dilution from accumulating moisture beneath the vegetation-free road, which was regularly sprinkled for dust control (Andraski et al., 2005). Moisture accumulation from devegetation alone was documented nearby (Andraski, 1997b; Johnson et al., 2007). Elevated concentrations south of the waste facility might also reflect a documented 1978 spill of liquid radioactive waste within the LLRW area that flowed to a location near the A-transect, 0-m sample site (ERM Program Management Co., personal communication, 1996).

Within 200 m of the LLRW facility, trends in $^3HHO_v$ concentrations at each location show that concentrations typically decreased from the sub-root-zone gravel to the root-zone soil, from the root-zone soil to plants, and from plants to canopy air (Fig. 3). The associated sub-root-zone concentrations along the Y650 transect exceeded root-zone concentrations by a factor of three or less, while A-transect sub-root-zone concentrations exceeded root-zone concentrations by a factor of two to five. These results are consistent with those reported by Andraski et al. (2005), who concluded that preferential lateral movement of $^3HHO_v$ from the waste source occurred through the coarse-textured sub-root-zone layer with concurrent upward movement into the root zone. Lateral and vertical differences between Y650- and A-transect concentrations might be due to differences in the composition of mixed waste sources west and south of the LLRW facility and to possible heterogeneities in soil properties controlling lateral and vertical subsurface transport. Root-zone soil $^3HHO_v$ concentrations exceeded plant $^3HHO_v$ concentrations by a factor of 3, on average, at sites within 200 m of the waste facility. The typically lower plant concentrations might be due in part to the exchange of ^3HHO between plant leaves and the surrounding water vapor of the atmosphere (Raney and Vaadia, 1965).

Replicated (n = 2) plant sampling allowed the effect of location on plant $^3HHO_v$ concentrations to be tested statistically within each transect and quarter. A logarithmic transformation was applied to the $^3HHO_v$ concentration data before statistical analyses. The ANOVA showed that the location effect within each transect and quarter was significant ($P > F < 0.0001$). In all cases, mean plant concentrations measured within 200 m of the waste

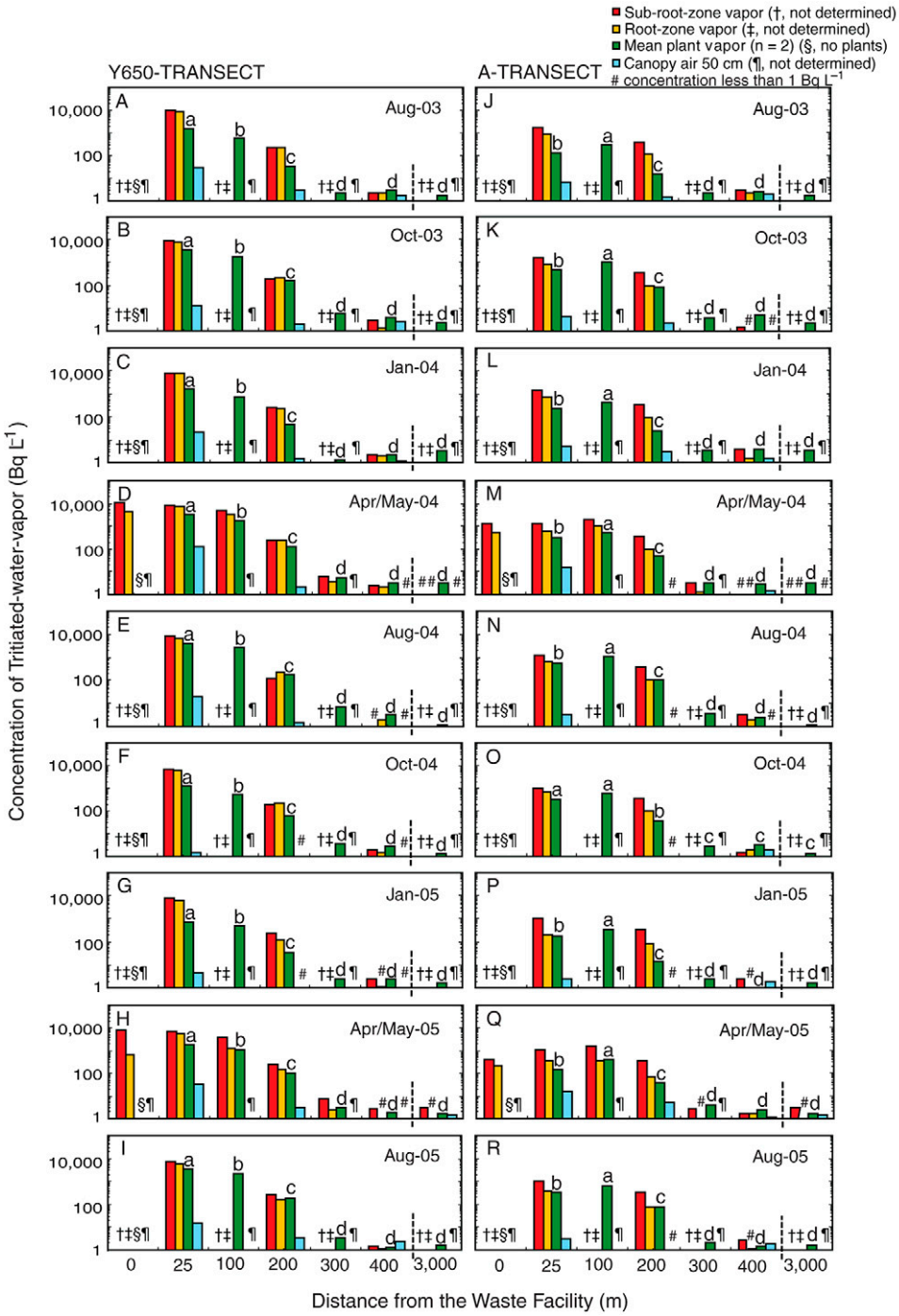

FIG. 3. Quarterly measured tritiated water vapor concentrations (logarithmic scale) with distance from the low-level radioactive waste facility along (A–I) Y650 and (J–R) A transects shown in Fig. 2, and at a distant (background) sample site 3000 m from the facility for the period of August 2003 to August 2005. Concentrations displayed are corrected for decay to the time of collection. No plants were present at the 0-m distance location. Mean plant concentrations within a given transect and quarter followed by the same letter (a–d) are not statistically different ($P < 0.05$), as determined by Fisher's least significant difference test.

facility were significantly greater than those measured beyond 200 m (Fig. 3A–3R). Plant concentrations measured at 300 and 400 m were not significantly different from background levels at the 3000-m distance. Stable quarter-to-quarter concentration trends along both transects indicate that the spatial distribution of $^3HHO_v$ concentrations varied little with time.

Elevated $^3HHO_v$ concentrations in canopy air support the occurrence of a measurable ^3H flux from the subsurface to the atmosphere. Canopy-air $^3HHO_v$ concentrations measured within 200 m of the waste facility were 97% less than plant concentrations, on average, and were consistently greatest 25 m from the LLRW facility (Fig. 3). The maximum canopy air concentration measured along the Y650 transect was 120 Bq L^{-1} (April–May 2004, 25 m from the facility); the maximum along the A transect was 15 Bq L^{-1} (April–May 2005, 25 m from the facility). Concentrations measured 200 m from the waste facility exceeded those measured at 400 m by a factor of 3 on average; concentrations measured 400 m from the facility were generally similar to background concentrations. The spatial differences in canopy-air concentrations corresponded with those in plant and root-zone water.

Temporal changes in soil and plant $^3HHO_v$ concentrations measured quarterly at the 25- and 200-m transect locations are shown in Fig. 4 along with precipitation and soil water content data. Sub-root-zone $^3HHO_v$ concentrations measured within 25 m of the waste facility showed long-term decreases that are greater than can be attributed to radioactive decay (Fig. 4A and 4D). In contrast, sub-root-zone concentration trends at sites 200 m from the waste facility showed little, if any, long-term decrease (Fig. 4B and 4E). Given that previous studies have identified the sub-root-zone gravelly sand as a preferential pathway for lateral transport of ^3H (Andraski et al., 2005), the difference in sub-root-zone temporal concentration trends between the 25- and 200-m sampling sites suggests movement of the $^3HHO_v$ plume with time. Concentration trends indicate that the portion of the $^3HHO_v$ plume within 25 m of the waste facility has reached peak concentrations and is now declining, while the portion of the plume located 200 m from the facility is still approaching peak values.

Long-term trends in root-zone soil $^3HHO_v$ concentrations generally corresponded with those observed in the sub-root-zone, but the root-zone concentrations also were subject to shorter term variations driven by dynamic processes within the root zone. A previous 5-yr study at the ADRS, which included daily water potential measurements, documented rapid penetration of precipitation to depths of 60 to 75 cm (attributed to flow along preferential paths) (Andraski, 1997b). Such percolation events would lead to rapid changes in ambient root-zone $^3HHO_v$ concentrations. The subsurface measurements made in the present study were not sufficient to capture all the dynamics of this mixing, but correlation analyses of quarterly data identified negative relations between root-zone soil $^3HHO_v$ concentrations and soil water contents at the 75-cm depth, providing evidence of percolation-induced dilution of root-zone $^3HHO_v$. The removal of dilute, freshly percolated water by evapotranspiration, equilibration with ambient soil water, and continued upward movement of higher ^3H-concentration water from the sub-root zone all contribute to a rebound in root-zone concentrations following infiltration events. Another process that mixes fresh (low-^3H) with ambient (high-^3H) water in the root zone is hydraulic redistribution by plants. Hydraulic redistribution can rapidly move water from moist to dry soil via plant root systems. The direction of movement is dictated by the prevailing soil water potential gradient and can be upward, downward, or horizontal (Caldwell et al., 1998; Scott et al., 2008). Yoder and Nowak (1999a) showed that at least three of the four shrub species at the ADRS (creosote-bush, burrobush, and wolfberry) provide conduits for hydraulic redistribution. Hydraulic redistribution is probably an active mechanism of mixing ^3HHO of varying concentrations within the root zone.

Plant $^3HHO_v$ concentrations showed relatively high variability but no long-term trends (Fig. 4A, 4B, 4D, and 4E). The quarter-to-quarter variability was greater for the plant concentrations (CV = 47–65%) than for the root-zone and sub-root-zone soil concentrations (CV = 5–38%). Yearly maximum plant $^3HHO_v$ values at a given location varied little from year to year.

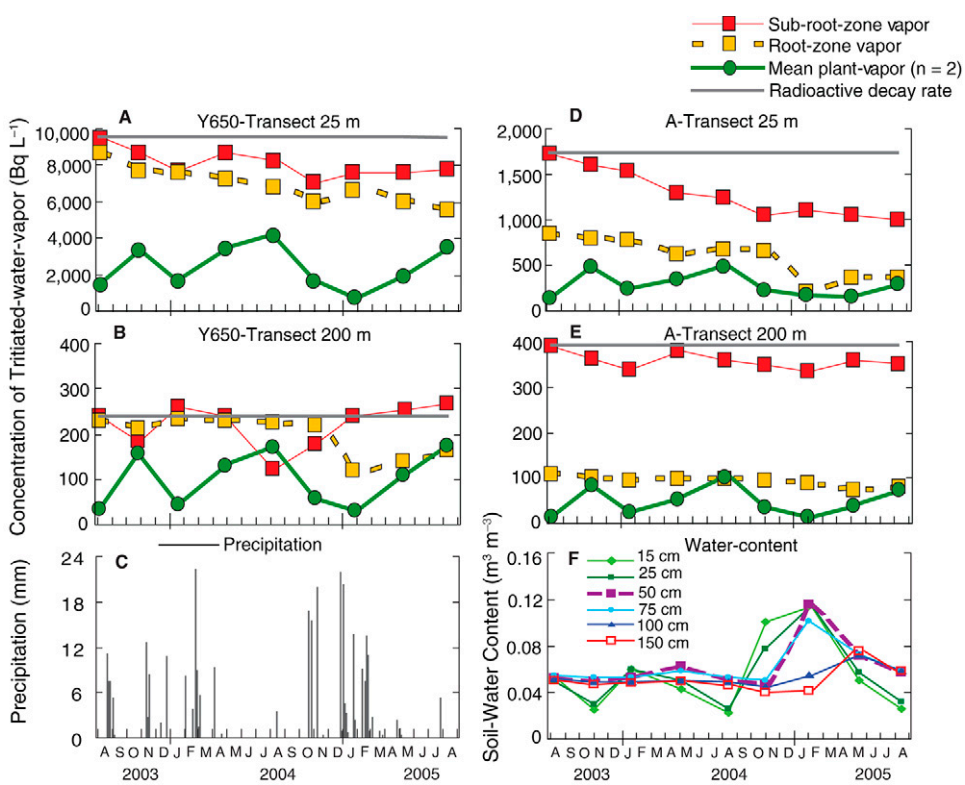

FIG. 4. Temporal changes in tritiated water vapor concentrations for locations 25 and 200 m from the waste disposal facility (Y650 and A transects), and temporal changes in precipitation and soil water content measurements at 15-, 25-, 50-, 75-, 100-, and 150-cm depths. Concentrations are corrected for decay to the time of collection.

Their timing corresponded with periods when root-zone water storage was at a minimum (October 2003, August 2004, and August 2005). The yearly minimum plant $^3HHO_v$ values for a given location also were fairly consistent from year to year even though they were measured under widely varying root-zone soil water storage conditions (August 2003, 5.3 cm; January 2004, 5.5 cm; and January 2005, 10.4 cm). These results indicate that dynamic processes in the plant environment generate short-term variability while buffering long-term trends.

Tritiated Water Vapor Concentration Distributions

Spatial distributions of $^3HHO_v$ concentrations in plants and root-zone soil for August 2003 are shown in Fig. 5. The linear regression equation developed to relate May 2001 and August 2003 plant $^3HHO_v$ concentrations and then applied to generate the August 2003 plant $^3HHO_v$ concentration map had an $r^2 = 0.99$ and was highly significant ($P < 0.01$). A similar, strong relation was observed for the linear regression equation used to create the August 2003 root-zone soil $^3HHO_v$ map ($r^2 = 0.95$, $P < 0.01$). The August 2003 maps (Fig. 5) show two localized hotspots of elevated $^3HHO_v$ concentrations west and south of the LLRW facility, indicating that the structure of these plumes was consistent with transect data and statistics shown in Fig. 3A and 3J, respectively. Concentrations estimated for off-transect locations were not verified with measured data, but were assumed to increase or decrease with quarterly measured transect data.

The spatial pattern in transect data (Fig. 3) remained consistent for all remaining quarters and, therefore, the overall structure of the mapped 2003 to 2005 plant and soil concentration distributions remained consistent with the May 2001 base map. The linear regression equations used to develop $^3HHO_v$ concentration maps for each of the remaining quarters were also highly significant ($P < 0.01$) and explained >96 and 88% of the variation in plant and root-zone soil data, respectively.

Evaporation and Transpiration

Continuously measured ET, partitioned E and T, and daily precipitation are shown in Fig. 6A and 6B. Evaporation ranged from 2 to 2430 g m^{-2} d^{-1} and transpiration ranged from 0.4 to 1610 g m^{-2} d^{-1}. The ET fluxes did not exhibit a strong seasonal pattern; rather, large increases occurred in response to precipitation. For example, the rise in E and T during February and March 2004 corresponded with a 10-d period with 41 mm of precipitation; another large and more sustained increase in E and T occurred during October to November 2004 when 66 mm of precipitation fell during a 21-d period (Fig. 6A and 6B).

Evaporation typically dominated the ET flux, but E/T values varied greatly. The 2-yr mean daily E/T ratio was 75:25; maximum and minimum daily ratios were 99.8:0.2 and 0.3:99.7, respectively. A similar mean daily E/T ratio (72:28) was computed using periodic chamber measurements (as described in Appendix B). The E/T partitioning reported here was within 10 to 15% of partitioning estimated from a 10-yr lysimeter study at the Nevada Test Site located about 70 km to the east (Scanlon et al., 2005). In that study, the mean monthly E/T ratio was about 85:15. Differences between our mean ratios and that for the lysimeter study probably stem in part from differences in experimental details. Evaporation measurements used to partition ET in the lysimeter study were made in a bare-soil lysimeter that was devoid of roots and therefore lacked subsurface root water uptake (Scanlon et al., 2005). In contrast, evaporation measurements used to partition ET at the ADRS were made in plant-interspace areas where, although the soil was bare, laterally extensive roots were present to extract moisture from beneath the bare surfaces (Yoder and Nowak, 1999b).

Tritium Transport

Daily study-area (0.76 km^2) fluxes of ^3H from the subsurface to the atmosphere are shown in Fig. 6C and ranged from 10^{-4} to 10^{-2} mg d^{-1}. The ^3H fluxes were quantified by combining daily plant and root-zone soil $^3HHO_v$ concentration maps with continuous E and T fluxes. Weather patterns dynamically affected intra- and interannual processes controlling ^3H flux magnitudes and variability. The ^3H fluxes were typically greater during periods of high ET and lower during periods of low ET (Fig. 6A and 6C). Intraannual evaluation indicates that variations in both ET and $^3HHO_v$ concentrations affected the ^3H flux. For example, the average daily ET flux for the period of February to March 2004 (935 g m^{-2} d^{-1}) was within 7% of that for the period of October to November 2004 (1007 g m^{-2} d^{-1}). In contrast, the average daily ^3H flux for February to March 2004 (4.4 μg m^{-2} d^{-1}) was 32% greater than that for October to November 2004 (3.0 μg m^{-2} d^{-1}). This lower ^3H flux primarily resulted from the precipitation-induced decrease in root-zone soil concentrations (about 10% on average) and an increase in the proportion of ET attributed to T. The average E/T ratio changed from 85:15 (February–March 2004) to 67:33 (October–November 2004) and the E/T ^3H flux ratio changed from 95:5 to 86:14 (Fig. 6A and 6C).

A comparison of the average daily ^3H flux for the periods of June to July 2004 and June to July 2005 also highlights the

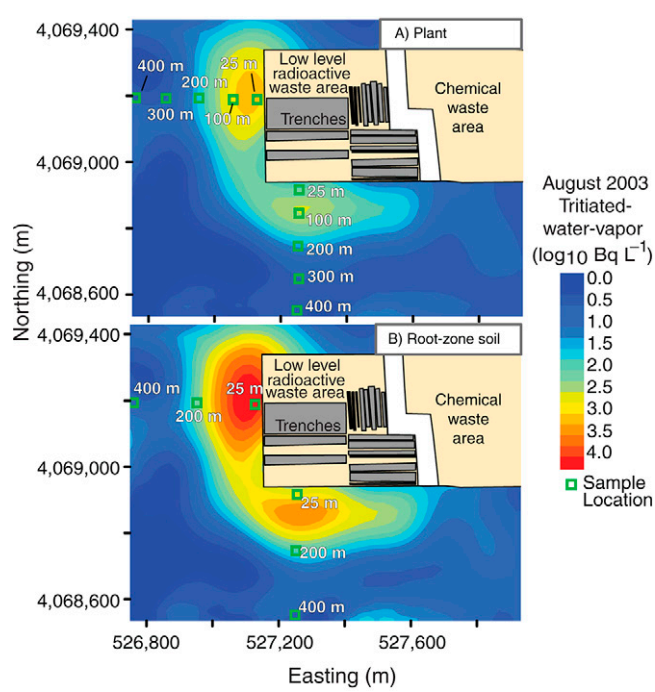

FIG. 5. Maps of tritiated water vapor concentrations in (A) plants and (B) root-zone soil for August 2003 and plant and soil sampling locations. Concentrations less than about 0.5 ($\log_{10}$ Bq L^{-1}) represent background levels.

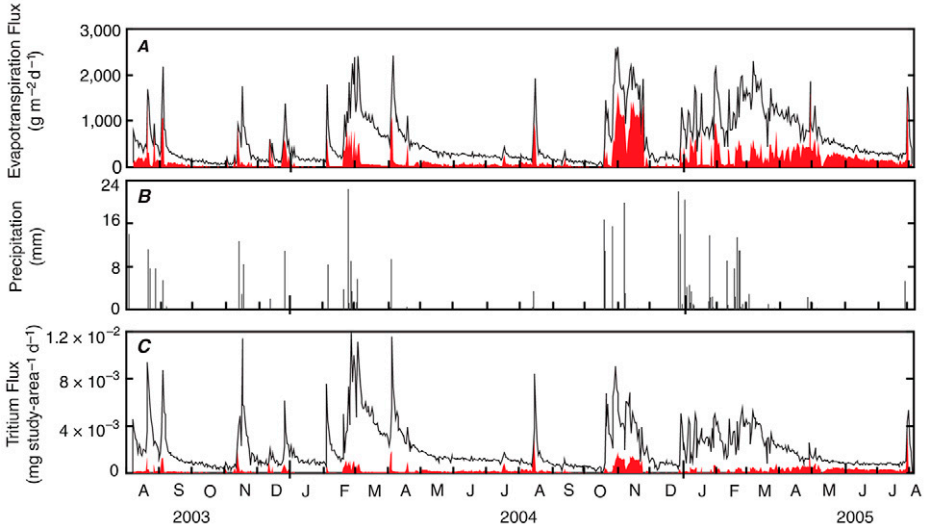

FIG. 6. Continuous (A) eddy-covariance evapotranspiration, (B) precipitation, and (C) tritium flux to the atmosphere from the 0.76-km^2 study area adjacent to the waste disposal facility. In (A) and (C), the colored portion of the total flux represents the transpiration component.

effects of dilution and partitioning between *E*- and *T*-generated ^{3}H fluxes. The average ET flux increased by 46% from June and July 2004 to June and July 2005 while the mean ^{3}H flux decreased by 16%. On average, the June and July 2005 root-zone soil concentrations were about 40% less than those for 2004 and the *E*/*T* ratios for these two periods changed from 78:22 to 54:46, respectively (Fig. 6A). In combination these factors contributed to *E*/*T* ^{3}H flux ratios that changed from 86:14 (June–July 2004) to 64:36 (June–July 2005) (Fig. 6C).

Evaluations of interannual fluxes showed that the annual mass of ET-derived ^{3}H released to the atmosphere decreased by about 14% from 0.82 mg in Year 1 (August 2003–August 2004) to 0.71 mg in Year 2 (August 2004–August 2005); decay corrections reduce this difference by 5%. Although ET increased from Year 1 to Year 2 (172,000 vs. 264,000 g m^{-2} yr^{-1}), increased precipitation (136 vs. 233 mm yr^{-1}) and resultant decreases in root-zone soil ^{3}HHO$_v$ concentrations (about 37% on average) reduced the annual mass of ^{3}H released to the atmosphere. For Years 1 and 2, respectively, the average *E*/*T* ratio changed from 81:19 to 69:31 and the *E*/*T* ^{3}H flux ratio changed from 92:8 to 81:19 (Fig. 6A and 6C).

The magnitude and distribution of the cumulative 2-yr ^{3}H flux to the atmosphere are shown in Fig. 7. The cumulative mass of ^{3}H released from areas adjacent to the LLRW facility during the 2-yr study was 1.5 mg (8.2 × 10^{10} Bq). Accounting for radioactive decay after emplacement into trenches (1962–1992), the mass released during the 2 yr represents 0.002% of the residual disposed ^{3}H. Exclusion of areas with background ^{3}HHO$_v$ concentrations (≤2.08 ± 1.35 Bq L^{-1}) from the analysis reduced the 2-yr mass released by <1%. The 2-yr flux distribution shown in Fig. 7 followed interpolated daily ^{3}HHO$_v$ concentration distributions, which remained relatively constant during the study period. Two-year ^{3}H flux magnitudes ranged from <10^{-8} (background) to 10^{-5} mg m^{-2} (within the western hotspot; Fig. 7). Areas near the western and southern hotspots that released 2-yr fluxes >10^{-6} mg m^{-2} represented <20% of the study area, but contributed to >90% of the total cumulative flux.

A general problem in developing monitoring and risk-assessment programs is the trade-off between the cost of data collection and the uncertainty in contaminant levels. To address this problem, we used subsets of our data to evaluate how reductions in the type or frequency of ^{3}HHO monitoring would affect estimates of the cumulative 2-yr ^{3}H flux to the atmosphere. In the first test, only quarterly measured root-zone soil ^{3}HHO$_v$ concentrations were used (without measured plant data) to estimate ^{3}H fluxes. This resulted in a cumulative 2-yr ^{3}H mass-flux estimate that was 25% greater than that for our previously described approach. In the second test, only quarterly measured plant concentrations were used (without measured soil gas data) to estimate ^{3}H fluxes. This resulted in a cumulative estimate that was 60% less than that for our approach. In the final test, requiring the least collection of data, only the August plant ^{3}HHO$_v$ concentrations in each year were used. The August plant ^{3}HHO$_v$ data were selected because differences between plant and root-zone soil ^{3}HHO$_v$ concentrations were typically lowest at that time. This test resulted in a cumulative flux estimate that was 30% less than that for our approach. Thus, depending on objectives, a simple strategy might be adequate. The reduction in type or frequency of data collection comes at the cost of greater uncertainty.

The main sources of uncertainty in ^{3}H flux calculations stem from the (i) empirical relations between May 2001 plant and August 2003 to August 2005 plant and root-zone ^{3}HHO$_v$ concentrations, (ii) interpolation of ^{3}HHO$_v$ concentrations between quarterly measurements, and (iii) concentration-gradient and barometric-pumping effects. Concentration estimates for off-transect locations were not verified with measured data. Even so, plume structures predicted from empirical relations south and west of the facility remained consistent with the spatial trends in measured concentrations—providing confidence in the empirical

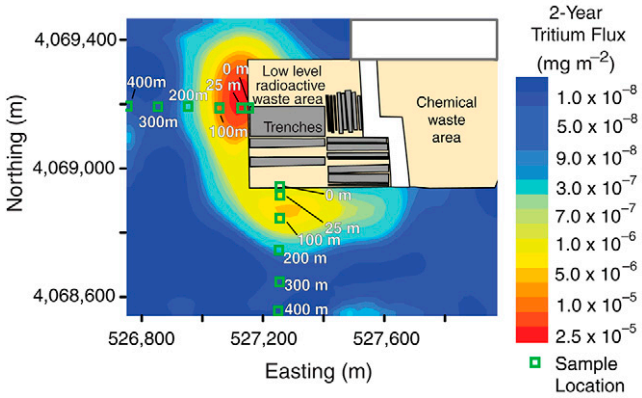

FIG. 7. Map of the cumulative 2-yr tritium flux (August 2003–August 2005) magnitude and distribution and plant and soil sampling locations adjacent to the waste disposal facility. Values less than or equal to about 1 × 10^{-8} mg m^{-2} represent background fluxes.

approach. Furthermore, the sampled transects nearly bisected the two areas that accounted for most of the ^3H flux. Interpolation of quarterly measured plant and root-zone soil $^3HHO_v$ concentrations missed shorter term (i.e., daily–monthly) changes that could occur in response to dynamic root-zone processes—e.g., concentration dilution by rapidly percolating water, concentration rebound as percolation water equilibrated with ambient soil water, and hydraulic redistribution by plants. Nonetheless, quarterly sampling did seem to adequately capture trends in plant and soil $^3HHO_v$ concentrations related to long-term changes in soil water content. Concentrations represent a lower frequency part of the signal compared with the continuously tracked ET fluxes. Perhaps the largest source of uncertainty is in the approximation of ^3H fluxes as simple products of partitioned ET water-vapor fluxes and $^3HHO_v$ concentrations, which ignores the effects of subsurface concentration gradients. If the dominant process is diffusion along a linear concentration gradient from high concentrations at depth to near-zero concentrations at the land surface, the amount of ^3H in evaporation will be much lower than the measured root-zone concentration, leading to an overestimate of the calculated evaporative ^3H flux. In contrast, evaporative enrichment at the evaporation surface could cause the concentration of ^3H in evaporation to be higher than the measured root-zone concentration, leading to an underestimate of the calculated evaporative ^3H flux (Allison, 1988). Minor additional effects arise because molecular interactions during multicomponent gas transport produce isotopic fractionation and counter flows (Thorstenson and Pollock, 1989; Evans et al., 2001). Finally, barometric pumping modifies transport compared with the purely diffusive case (Auer et al., 1996). At the ADRS, barometric pumping was estimated to accelerate the movement of gas-phase contaminants by as much as a factor of 10 over diffusion alone (Smith et al., 1999).

Implications for Remediation and Waste Disposal

Field-based results have important implications for remediation and contaminant transport near arid waste facilities. The 2-yr ^3H flux to the atmosphere from land adjacent to the LLRW facility represents a small but measurable amount of the total ^3H disposed in the waste trenches (0.002% of the amount remaining after decay, as of August 2003). As a first approximation of future long-term releases, the 2-yr measured flux was extrapolated forward through time. Assuming future releases decline at the rate of radioactive decay, the 40-yr (to August 2043) cumulative mass of ^3H that will have entered the atmosphere totals 13 mg. This value is roughly eight to nine times greater than the mass released during the 2-yr study and represents about 0.05% of the steadily diminishing inventory of disposed ^3H. Due to decay after release, the cumulative mass of ^3H added to the atmospheric reservoir (after August 2003) should reach a maximum of 5.6 mg in the year 2021 and decrease thereafter.

Evapotranspiration fluxes from a sparsely vegetated landscape (~6% plant cover) were shown to limit downward contaminant migration. Given that creosote-bush roots are laterally extensive and allow soil water uptake well beyond the aboveground plant canopy, plants can facilitate the depletion of short-term moisture accumulation throughout the root zone. Depletion of root-zone moisture prevented liquid penetration below the root zone, thereby limiting the potential for deep contaminant transport. Previous studies at the ADRS have documented negligible long-term moisture accumulation in root-zone soil and predominantly upward movement of water and ^3H beneath vegetated soils (Andraski, 1997b; Andraski et al., 2005; Johnson et al., 2007). Beneath actively devegetated soils, however, these studies have documented measurable long-term moisture accumulation within and below the root zone, prompting primarily downward $^3HHO_w$ flow.

Recognizing preferential vapor-phase movement of ^3HHO through the sub-root zone (Andraski et al., 2005), temporal trends in $^3HHO_v$ concentrations have important implications for lateral ^3H transport. Time series data document lateral migration of ^3H away from the waste facility. Sub-root-zone $^3HHO_v$ concentrations measured near the centroid of both the western and southern concentration hotspots generally decreased at rates greater than radioactive decay, suggesting that the peak concentrations have already occurred and contamination is moving away from this area. In contrast, concentrations measured at sites located 200 m from the waste facility increased or decreased at rates less than radioactive decay, suggesting that this position is consistent with the leading edge of an advancing (but decaying) plume.

Results from this and previous studies performed at the ADRS provide insight into the main factors and processes that affect contaminant transport at arid waste disposal facilities. For example, the removal of plants from trench covers during the operational period of LLRW disposal facilities together with the long time requirements for natural reestablishment of native plants on final covers enhance the accumulation of precipitation within the disposal area. This accumulation of moisture increases the potential for downward percolation and liquid transport of contaminants toward groundwater. An 18-yr (1987–2005) record of soil moisture monitoring collected under unvegetated simulated waste trench conditions at the ADRS documented such an accumulation of precipitation with time (Andraski, 1997b; Johnson et al., 2007). This record also showed that wetting front penetration was limited to a depth of <3 m, emphasizing the importance of gas-phase liquid transport in arid environments. The ADRS studies of vapor-phase transport from the LLRW facility have documented elevated $^3HHO_v$ concentrations throughout the deep unsaturated zone (e.g., Mayers et al., 2005).

Shallow moisture accumulation could also affect contaminant transport at an arid waste-disposal facility by impeding the upward gas-phase migration of contaminants through the trench cover or backfill that overlies buried waste. Such an impediment to the release of contaminants via upward emission to the atmosphere may play a role in the observed, but as yet unexplained, long-distance (hundreds of meters) lateral migration of $^3HHO_v$ and elemental Hg through the arid unsaturated zone at the ADRS (Andraski et al., 2005; Mayers et al., 2005; Walvoord et al., 2008).

In addition to the aforementioned factors and processes, the potential for downward liquid transport of contaminants at a waste-burial site is enhanced when precipitation and runoff collects in open trenches and when liquids are disposed directly into unlined trenches. Under such conditions, the effectiveness of natural arid-site waste-isolation features that can decrease the potential for groundwater contamination, such as low precipitation and high evaporative demand, are diminished.

Conclusions

This study documented the effects of soil–plant–atmosphere interactions on water-borne contaminant fluxes in an arid environment by quantifying 2 yr of ^3H transport from the shallow unsaturated zone to the atmosphere adjacent to a LLRW facility. Tritium fluxes were approximated as simple products of ET flux and ^3H concentration. The distribution of ^3H fluxes remained relatively constant during the study period and predominantly decreased with distance from the waste facility. Weather patterns dynamically affected intra- and interannual processes controlling ^3H flux magnitudes and temporal variability. Precipitation events were shown to promote dilution of root-zone soil $^3HHO_v$ concentrations and increase the proportion of ET attributed to transpiration. A combination of these factors ultimately led to the difference between ^3H fluxes in Year 1 (0.82 mg) and Year 2 (0.71 mg).

Remediation through desert ET was shown to remove a total ^3H mass of 1.5 mg (8.2×10^{10} Bq) from the 0.76-km^2 study area from August 2003 to August 2005; this mass equates to 0.002% of the initial ^3H disposed at the LLWR facility. Remediation through ET (218,000 g m^{-2} yr^{-1} on average) was greatest within the western hotspot where root-zone soil water vapor concentrations reached a maximum of 8700 Bq L^{-1}. Maximum ^3H removal rates in this area were 10^{-5} mg m^{-2} yr^{-1} (equivalent to 10^6 Bq m^{-2} yr^{-1}).

Evapotranspiration from sparsely vegetated soil was shown not only to remove and limit the penetration of precipitation but also to foster upward movement and release of ^3H from below the root zone. The temporal dynamics of the ^3H flux mirror those of the ET flux, which is driven by water availability. The rapid response of native vegetation to precipitation quickly boosts transpiration, greatly limiting deep percolation of infiltrating water. This, in turn, preserves hydrologic gradients promoting upward movement of ^3H from below the root zone and subsequent release to the atmosphere. Removing vegetation from the natural soil–plant–atmosphere continuum has been shown in companion studies to initiate soil moisture accumulation, which leads to downward hydraulic gradients and reduced ^3H fluxes to the atmosphere.

Desert plants play an important role in the shallow soil water balance, in the remediation of shallow water-borne contamination, and in deep unsaturated-zone water movement. To our knowledge, this study is the first to quantify naturally occurring remediation of a subsurface vapor-phase ^3H plume in an arid environment. In addition, the study delineated the evaporative and transpirative components of the soil–atmosphere ^3H flux, providing an improved understanding of processes controlling subsurface transport and release of contaminants to the atmosphere. Results of this study will be useful in testing and refining numerical models of ^3H transport and in evaluating transport pathways.

Appendix A: Evaporation Estimates Using the Priestley–Taylor Model

Evaporation estimates were based on the Priestley–Taylor model and the following equation (Davies and Allen, 1973):

$$\lambda E_{ss} = \alpha' \frac{S}{S+\gamma}\left(R_n - G\right) \qquad [A1]$$

where λE_{ss} is the site-scale latent heat flux (W m^{-2}), α' is the Priestley–Taylor coefficient dependent on micrometeorological data (unitless), S is the slope of the saturation vapor pressure–temperature curve (kPa °C^{-1}), γ is the psychrometric constant (kPa °C^{-1}), R_n is the net radiation (W m^{-2}), and G is the ground heat flux (W m^{-2}). The model was calibrated using quarterly measurements made periodically at 15-min intervals throughout a given day. Data included mean bare-soil λE_{ss} that was determined from 1-m-diameter hemispherical chamber (Stannard, 1988; Stannard and Weltz, 2006) measurements at two replicate sites (Garcia et al., 2008). Air temperature (T_a in °C) was measured and used to compute the second term on the right side of Eq. [A1] using a polynomial regression equation fitted to data from Shuttleworth (1993, Table 4.1.1) and adjusted for pressure changes with elevation (i.e., adjusted from sea level to the site elevation of 850 m):

$$\frac{S}{S+\gamma} = -0.00014T_a^2 + 0.169T_a + 0.411 \qquad [A2]$$

The R_n was measured using a net radiometer and G was the measured average for soil-heat-flux plates buried at a depth of 8 cm. Using these measured and calculated 15-min values, Eq. [A1] was solved for α'. A functional relation then was developed between α' and near-surface soil water content (averaged between 0- and 8-cm depths) measured using a water content reflectometer (Johnson et al., 2007):

$$\alpha' = f(\theta),\ 0 < \theta < \theta_{ns} \qquad [A3]$$

$$\alpha' = 1.26,\ \theta \geq \theta_{ns} \qquad [A4]$$

where θ is the water content (m^3 m^{-3}) and θ_{ns} is the water content near and at saturation. Equation [A3] was developed by regressing the calculated α' against near-surface soil water content. For near-saturated and saturated surfaces, a constant of 1.26 was substituted for α' (Eq. [A4]). This functional relationship was used to predict continuous α' from continuous θ measurements.

The final calibration data set relating computed α' to near-surface soil water content is shown in Fig. A1. Negative α' values from the initial data set were removed by excluding data collected during periods when solar radiation was low (<135 W m^{-2}; sunset to sunrise), similar to Flint and Childs (1991). The linear regression equation given in Fig. A1 relating α' to shallow soil water content follows a segmented linear model (Priestley and Taylor, 1972; Black, 1979) that includes a constant α' segment of 1.26 for soil water contents at and near saturation and a linear-model segment for soil water contents <0.26 m^3 m^{-3}.

In some cases, relatively large variations in α' were observed at virtually constant values of soil water content. This was attributed to (i) precipitation the day of or the day before bare-soil E measurements and (ii) near-surface soil water content measurements that recorded an average value for the 0- to 8-cm depth. For example, one set of α' values computed from micrometeorological measurements made shortly after 1.3 mm of precipitation decreased from 1.40 to 0.18 while the measured soil water content remained virtually constant at 0.046 ± 0.004 m^3 m^{-3}. These data indicate that the 0- to 8-cm soil water content measurements were not as dynamic as the surface-flux processes being measured by the hemispherical chamber following light precipitation.

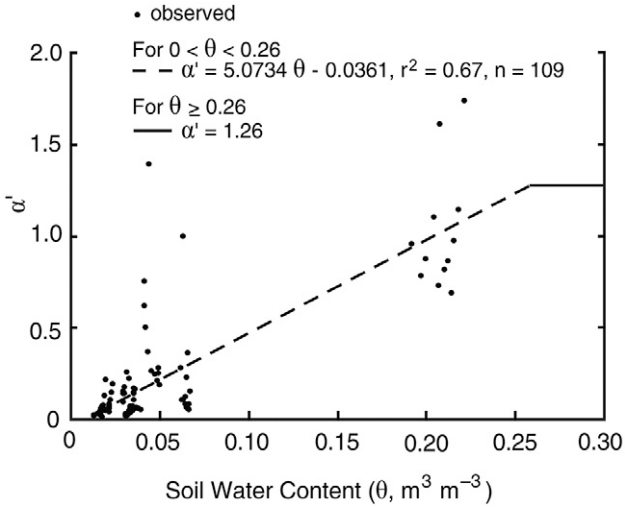

FIG. A1. Relation between the Priestley–Taylor coefficient (α') and soil water content (θ) used in the Priestley–Taylor model for estimation of continuous bare-soil evaporation (E_{ss} in Eq. [1] and [2]). Data are based on 15-min measurements made throughout the day on various dates during August 2003 to August 2005.

Appendix B: Comparison of Evapotranspiration Measurements Using Eddy-Covariance and a Hemispherical Chamber

A comparison between eddy-covariance and periodic hemispherical chamber ET measurements validated use of the chamber for partitioning continuously measured eddy-covariance ET into *E* and *T*. For this comparison, chamber ET measurements of bare soil and creosote-bush were merged to compute landscape-scale ET using a one-layer, two-component model (Stannard, 1988):

$$\overline{\mathrm{ET}} = \mathrm{Fc_p}\frac{\mathrm{ET_p} - \mathrm{ET_s}\left(1 - \mathrm{Rc_p}\right)}{\mathrm{Rc_p}} + \mathrm{Fc_s}\mathrm{ET_s} \qquad [B1]$$

where $\overline{\mathrm{ET}}$ is the mean landscape-scale ET (g m^{-2} d^{-1}), p represents plants, s represents bare soil, ET is the site-scale ET of plants or bare soil (g m^{-2} d^{-1}), and Rc is the chamber relative-shadow area (relative cover) of plants (unitless). The Rc value was determined by digitizing overhead photographs of plant cover within the 1-m-diameter chamber measurement area (Garcia et al., 2008).

Data comparing 15-min measurements of eddy-covariance ET and chamber ET are shown in Fig. B1. Paired eddy-covariance and hemispherical chamber measurements of ET were similar and unbiased. Correlation analysis showed a highly significant, positive relation between the two measurement methods (r = 0.857; $P > |r| < 0.0001$). With the exception of a single data pair (chamber ET = 2.4 g m^{-2} 15 min^{-1} and eddy-covariance ET = 0.06 g m^{-2} 15 min^{-1}, August 2004, 7:15 h) chamber ET was, on average, 3% greater than eddy-covariance ET. These results are well within the range of those for previous studies that reported similar correlation coefficients and slightly greater chamber ET than eddy-covariance ET (Dugas et al., 1991; Stannard and Weltz, 2006). The good agreement between the ET measurement techniques provided confidence that the chamber approach yielded reliable measurements of bare-soil *E* for partitioning continuously measured ET into *E* and *T* for the ^{3}H flux study.

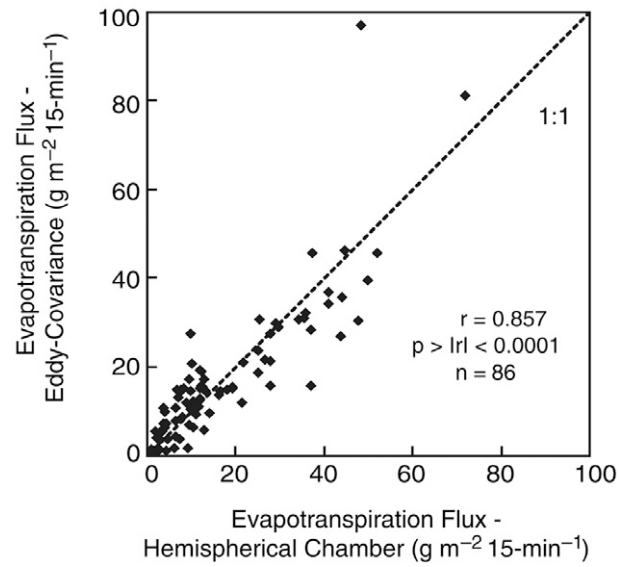

FIG. B1. Comparison of 15-min eddy-covariance evapotranspiration and hemispherical chamber evapotranspiration fluxes (bare-soil evaporation and creosote-bush transpiration), measured quarterly from August 2003 to August 2005 (1.0 g m^{-2} d^{-1} = 0.001 mm d^{-1}).

Acknowledgments

We gratefully acknowledge R.S. Nowak for extensive cooperation and assistance in use of his laboratory for toluene extractions. We also thank C.J. Mayers and R.J. Baker for field and laboratory assistance; D.I. Stannard, M.A. Walvoord, and K.J. Halford for helpful comments on the manuscript; and K.J. Halford for improving data processing efficiency. The manuscript was additionally improved by constructive criticism from P.H. Stauffer and anonymous reviewers. Support for this work was provided through the USGS's Toxic Substances Hydrology, National Research, and Ground-Water Resources programs.

References

Allison, G.B. 1988. A review of some of the physical, chemical and isotopic techniques available for estimating ground water recharge. p. 49–72. *In* I. Simmers (ed.) Estimation of natural ground water recharge. NATO Adv. Sci., Ser. C Math. Phys. Sci. 222. D. Reidel Publ. Co., Dordrecht, the Netherlands.

Andraski, B.J. 1996. Properties and variability of soil and trench fill at an arid waste-burial site. Soil Sci. Soc. Am. J. 60:54–66.

Andraski, B.J. 1997a. Test-trench studies in the Amargosa Desert, southern Nevada: Results and application of information to landfill covers in arid environments. p. 165–179. *In* T.D. Reynolds and R.C. Morris (ed.) Proc. Landfill Capping in the Semi-arid West: Problems, Perspectives, and Solutions, Jackson Lake Lodge, WY. 21–22 May 1997. ESRF-019. Environ. Sci. and Res. Found., Idaho Falls, ID.

Andraski, B.J. 1997b. Soil-water movement under natural-site and waste-site conditions: A multiple-year field study in the Mojave Desert, Nevada. Water Resour. Res. 33:1901–1916.

Andraski, B.J., M.W. Sandstrom, R.L. Michel, J.C. Radyk, D.A. Stonestrom, M.J. Johnson, and C.J. Mayers. 2003. Simplified method for detecting tritium contamination in plants and soil. J. Environ. Qual. 32:988–995.

Andraski, B.J., D.A. Stonestrom, R.L. Michel, K.J. Halford, and J.C. Radyk. 2005. Plant-based plume-scale mapping of tritium contamination in desert soils. Vadose Zone J. 4:819–827.

Auer, L.H., N.D. Rosenberg, K.H. Birdsell, and E.M. Whitney. 1996. The effects of barometric pumping on contaminant transport. J. Contam. Hydrol. 24:145–166.

Black, T.A. 1979. Evapotranspiration from Douglas-fir stands exposed to soil water deficits. Water Resour. Res. 15:164–170.

Caldwell, M.M., T.E. Dawson, and J.H. Richards. 1998. Hydraulic lift: Consequences of water efflux from the roots of plants. Oecologia 113:151–161.

Davies, J.A., and C.D. Allen. 1973. Equilibrium, potential and actual evaporation from cropped surfaces in southern Ontario. J. Appl. Meteorol. 12:649–657.

Dugas, W.A., L.J. Fritschen, L.W. Gay, A.A. Held, A.D. Matthias, D.C. Reicosky, P. Steduto, and J.L. Steiner. 1991. Bowen ratio, eddy correlation, and portable chamber measurements of sensible and latent heat flux over irrigated spring wheat. Agric. For. Meteorol. 56:1–20.

Evans, W.C., M.L. Sorey, B.M. Kennedy, D.A. Stonestrom, J.D. Rogie, and D.L. Shuster. 2001. High CO_2 emissions through porous media: Transport mechanisms and implications for flux measurement and fractionation. Chem. Geol. 177:15–29.

Fernandez, G.C.J. 1992. Residual analysis and data transformations: Important tools in statistical analysis. Hortic. Sci. 27:297–300.

Ferronsky, V.I., and V.A. Polyakov. 1982. Environmental isotopes in the hydrosphere. John Wiley & Sons, New York.

Fischer, J.M. 1992. Sediment properties and water movement through shallow unsaturated alluvium at an arid site for disposal of low-level radioactive waste near Beatty, Nye County, Nevada. USGS Water Resour. Invest. Rep. 92-4032. USGS, Denver, CO.

Flint, A.L., and S.W. Childs. 1991. Use of the Priestley–Taylor evaporation equation for soil water limited conditions in a small forest clearcut. Agric. For. Meteorol. 56:247–260.

Garcia, C.A. 2007. Vertical tritium transport from the shallow unsaturated zone to the atmosphere, Amargosa Desert Research Site, Nevada. M.S. thesis. Univ. of Nevada, Reno.

Garcia, C.A., M.J. Johnson, B.J. Andraski, K.J. Halford, and C.J. Mayers. 2008. Portable chamber measurements of evapotranspiration at Amargosa Desert Research Site in Nye County near Beatty, Nevada. Available at pubs.usgs.gov/sir/2008/5135 (accessed 22 Dec. 2008, verified 24 Jan. 2009). USGS Sci. Invest. Rep. 2008-5135. USGS, Denver, CO.

Gile, L.H., R.P. Gibbens, and J.M. Lenz. 1998. Soil-induced variability in root systems of creosotebush (*Larrea tridentata*) and tarbush (*Flourensia cernua*). J. Arid Environ. 39:57–78.

Johnson, M.J., C.J. Mayers, C.A. Garcia, and B.J. Andraski. 2007. Selected micrometeorological, soil moisture and evapotranspiration data at Amargosa Desert Research Site in Nye County near Beatty, Nevada, 2001–2005. Available at pubs.water.usgs.gov/ds284 (accessed 21 Feb. 2008, verified 24 Jan. 2009). Data Ser. 284. USGS, Denver, CO.

Kalisz, P.J., J.W. Stringer, J.A. Volpe, and D.T. Clark. 1988. Trees as monitors of tritium in soil water. J. Environ. Qual. 17:62–70.

Kwicklis, E.M., A.V. Wolfsberg, P.H. Stauffer, M.A. Walvoord, and M.J. Sully. 2006. Multiphase multicomponent parameter estimation for liquid and vapor fluxes in deep arid systems using hydrologic data and natural environmental tracers. Vadose Zone J. 5:934–950.

Mayers, C.J., B.J. Andraski, C.A. Cooper, S.W. Wheatcraft, D.A. Stonestrom, and R.L. Michel. 2005. Modeling tritium transport through a deep unsaturated zone in an arid environment. Vadose Zone J. 4:967–976.

Negri, M.C., R. Hinchman, and J. Wozniak. 2000. Capturing a mixed contaminant plume: Tritium phytoevaporation at Argonne National Laboratory at Area 319. p. 189–198. *In* Phytoremediation: State of the Science Conf., Boston, MA. 1–2 May 2000. USEPA, Boston, MA.

Nichols, W.D. 1987. Geohydrology of the unsaturated zone at the burial site for low-level radioactive waste near Beatty, Nye County, Nevada. Water-Supply Pap. 2312. USGS, Denver, CO.

Phillips, F.M. 1994. Environmental tracers for water movement in desert soils of the American Southwest. Soil Sci. Soc. Am. J. 58:15–24.

Priestley, C.H.B., and R.J. Taylor. 1972. On the assessment of surface heat flux and evaporation using large-scale parameters. Mon. Weather Rev. 100:81–92.

Raney, F., and Y. Vaadia. 1965. Movement and distribution of THO in tissue water and vapor transpired by shoots of *Helianthus* and *Nicotiana*. Plant Physiol. 40:383–388.

Revesz, K., and P.H. Woods. 1990. A method to extract soil water for stable isotope analysis. J. Hydrol. 115:397–406.

Rickard, W.H., and L.J. Kirby. 1987. Trees as indicators of subterranean water flow from a retired radioactive waste disposal site. Health Phys. 52:201–206.

Rickard, W.H., and K.R. Price. 1989. Uptake of tritiated groundwater by black locust trees. Northwest Sci. 63:87–89.

SAS Institute. 2001. SAS/STAT software. Release 8.2. SAS Inst., Cary, NC.

Scanlon, B.R., K. Keese, R.C. Reedy, J. Šimůnek, and B.J. Andraski. 2003. Variations in flow and transport in thick desert vadose zones in response to paleoclimatic forcing (0–90 kyr): Field measurements, modeling, and uncertainties. Water Resour. Res. 39(7):1179, doi:10.1029/2002wr001604.

Scanlon, B.R., D.G. Levitt, R.C. Reedy, K.E. Keese, and M.J. Sully. 2005. Ecological controls on water-cycle response to climate variability in deserts. Proc. Natl. Acad. Sci. 103:6033–6038.

Scanlon, B.R., and P.C.D. Milly. 1994. Water and heat fluxes in desert soils: 2. Numerical simulations. Water Resour. Res. 30:721–733.

Scott, R.L., W.L. Cable, and K.R. Hultine. 2008. The ecohydrologic significance of hydraulic redistribution in a semiarid savanna. Water Resour. Res. 44:W02440, doi:10.1029/2007wr006149.

Shuttleworth, J.W. 1993. Evaporation. p. 4.1–4.53. *In* D.R. Maidment (ed.) Handbook of hydrology. McGraw-Hill, New York.

Smith, R.L. 1974. Ecology and field biology. 2nd ed. Harper and Row, New York.

Smith, S.D., R.K. Monson, and J.E. Anderson. 1997. Physiological ecology of North American desert plants. Springer-Verlag, Berlin.

Smith, T.R., D.A. Stonestrom, and D.E. Prudic. 1999. Barometric pumping in a 110-meter thick unsaturated zone in the Amargosa Desert, Nye County, Nevada. Eos Trans. Am. Geophys. Union 80(46):F359.

Stannard, D.I. 1988. Use of a hemispherical chamber for measurement of evapotranspiration. Open-File Rep. 88-452. USGS, Denver, CO.

Stannard, D.I., and M.A. Weltz. 2006. Partitioning evapotranspiration in sparsely vegetated rangeland using a portable chamber. Water Resour. Res. 42:W02413, doi:10.1029/2005WR004251.

Steel, R.G., and J.H. Torrie. 1980. Principles and procedures of statistics. McGraw-Hill, New York.

Striegl, R.G. 1988. Distribution of gases in the unsaturated zone at a low-level radioactive-waste disposal site near Sheffield, Illinois. Water Resour. Invest. Rep. 88-4025. USGS, Denver, CO.

Striegl, R.G., D.E. Prudic, J.S. Duval, R.W. Healy, E.R. Landa, D.W. Pollock, D.C. Thorstenson, and E.P. Weeks. 1996. Factors affecting tritium and carbon-14 distributions in the unsaturated zone near the low-level radioactive-waste burial site south of Beatty, Nevada. Open-File Rep. 96–110. USGS, Denver, CO.

Thatcher, L.L., V.J. Janzer, and K.W. Edwards. 1977. Methods for determination of radioactive substances in water and fluvial sediments. Ch. A5. *In* USGS Techniques of Water Resources Investigations, Book 5. U.S. Gov. Print Office, Washington, DC.

Thorstenson, D.C., and D.W. Pollock. 1989. Gas transport in unsaturated porous media: The adequacy of Fick's law. Rev. Geophys. 27:61–78.

U.S. Nuclear Regulatory Commission. Office of Inspection and Enforcement, Region V. 1976. IE Inspection Rep. 76–02. U.S. Nuclear Regulatory Commission Region V, Walnut Creek, CA.

Walvoord, M.A., B.J. Andraski, D.P. Krabbenhoft, and R.G. Striegl. 2008. Transport of elemental mercury in the unsaturated zone from a waste disposal site in an arid region. Appl. Geochem. 23:572–583.

Walvoord, M.A., M.A. Plummer, F.M. Phillips, and A.V. Wolfsberg. 2002. Deep arid system hydrodynamics: 1. Equilibrium states and response times in thick desert vadose zones. Water Resour. Res. 38(12):1308, doi:10.1029/2001WR000824.

Walvoord, M.A., D.A. Stonestrom, B.J. Andraski, and R.G. Striegl. 2004. Constraining the inferred paleohydrologic evolution of a deep unsaturated zone in the Amargosa Desert. Vadose Zone J. 3:502–512.

Yoder, C.K., and R.S. Nowak. 1999a. Hydraulic lift among native plant species in the Mojave Desert. Plant Soil 215:93–102.

Yoder, C.K., and R.S. Nowak. 1999b. Soil moisture extraction by evergreen and drought-deciduous shrubs in the Mojave Desert during wet and dry years. J. Arid Environ. 42:81–96.